ACS BIO & MED CHEM Au
AN OPEN ACCESS JOURNAL OF THE AMERICAN CHEMICAL SOCIETY

pubs.acs.org/biomedchemau
Article

Metabolic Probing of Sialylated Glycoconjugates with Fluorine-Selenol Displacement Reaction (FSeDR)

Published as part of ACS Bio & Med Chem Au special issue "2024 Rising Stars in Biological, Medicinal, and Pharmaceutical Chemistry".

Yue Zhao,[†] Zhigang Lyu,[†] Benjamin Prather, Todd R. Lewis, Jinfeng Kang, and Rongsheng E. Wang*

Cite This: ACS Bio Med Chem Au 2025, 5, 119−130
Read Online

ACCESS | Metrics & More | Article Recommendations | Supporting Information

ABSTRACT: Dysregulated sialic acid biosynthesis is characteristic of the onset and progression of human diseases including hormone-sensitive prostate cancer and breast cancer. The sialylated glycoconjugates involved in this process are therefore important targets for identification and functional studies. To date, one of the most common strategies is metabolic glycoengineering, which utilizes *N*-acetylmannosamine (ManNAc) analogues such as *N*-azidoacetylmannosamine (ManNAz) to hijack sialic acid biosynthesis and label the sialylated glycoconjugates with "click chemistry (CuAAC)" tags. Yet, current chemical modifications including those CuAAC-based alkyne/azide tags are still big in size, and the resulting steric hindrance perturbs the mannosamine and sialic acid derivatives' recognition and metabolism by enzymes involved in biosynthetic pathways. As a result, the peracetylated ManNAz has compromised incorporation to sialic acid substrates and manifests cellular growth inhibition and cytotoxicity. Herein, we show that the α-fluorinated peracetylated analogue ManN(F-Ac) displayed a satisfying safety profile in mammalian cell lines at concentrations as high as 500 μM. More importantly, aliphatic selenol-containing probes can efficiently displace α-fluorine in fluoroacetamide-containing substrates including ManN(F-Ac) at a neutral pH range (~7.2). The combined use of peracetylated ManN(F-Ac) and the dethiobiotin-selenol probe as the fluorine-selenol displacement reaction (FSeDR) toolkit allowed for successful metabolic labeling of sialoglycoproteins in multiple prostate and cancer cell lines, including PC-3 and MDA-MB-231. More sialoglycoproteins in these cell lines were demonstrated to be labeled by FSeDR compared with the traditional CuAAC approach. Lastly, with FSeDR-mediated metabolic labeling, we were able to probe the cellular expression level and spatial distribution of sialylated glycoconjugates during the progression of these hormone-sensitive cancer cells. Taken together, the promising results suggest the potential of the FSeDR strategy to efficiently and systematically identify and study sialic acid substrates and potentially empower metabolic engineering on a diverse set of glycosylated proteins that are vital for human diseases.

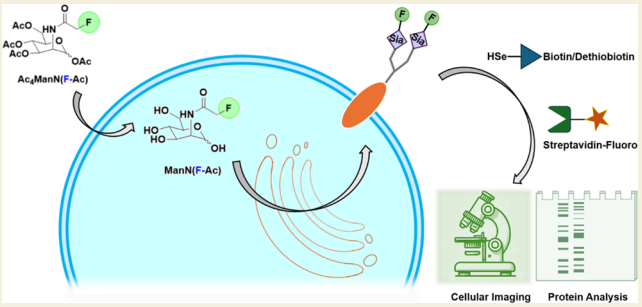

KEYWORDS: *metabolic engineering, mannosamine, sialic acid, glycobiology, fluorine displacement reaction, selenium, fluorine-selenol displacement reaction (FSeDR)*

INTRODUCTION

Sialic acids are a family of α-keto acid carbohydrates with a nine-carbon backbone, such as *N*-acetylneuraminic acid,[1] which are synthesized intracellularly and incorporated by sialyltransferases onto protein substrates in the Golgi.[2] The resulting sialylated glycoconjugates are eventually transported to cell surfaces[2] and are typically found at the termini of cell surface glycan chains. Sialoglycoproteins mediate various recognition processes,[3] cell−cell interactions,[3] and host−pathogen interactions.[2] Dysregulation of sialic acid biosynthesis was observed to be pivotal not only to genetic diseases such as GNE myopathy but also many other human diseases including cancer and inflammatory disorders.[1,4] Thus, it is important to understand the glycan biology involved with the substrates in the sialic acid biosynthesis pathway, particularly in different disease settings.

Metabolic glycoengineering represents an established chemical biology method that enables the visualization and isolation of glycans for probing their biological roles.[3,5] More recently, metabolic labeling of dysregulated glycans such as sialic acids on cancer cells also emerged for targeted

Received: August 27, 2024
Revised: November 27, 2024
Accepted: December 2, 2024
Published: December 9, 2024

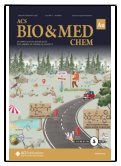

treatment.[6] Such metabolic glycoengineering strategies typically utilize *N*-acetylmannosamine (ManNAc) derivatives that have been modified with chemical reporters.[5,7−9] The most common tool is *N*-azidoacetylmannosamine (ManNAz) in its peracetylated form to improve cell permeability,[5] which is metabolized intracellularly, hijacking the involved enzymes in the sialic acid biosynthesis, and eventually converted to *N*-azidoacetylneuraminic acid (Neu5Az).[2] The azido reporter group can then be utilized as a bioorthogonal handle on sialylated glycoconjugates,[2] to be later appended via "click chemistry (CuAAC)"[5] with a fluorophore for imaging or a biotin affinity tag for enrichment and functional studies. Success in hijacking this sugar salvage pathway usually requires the involved enzymes to be promiscuous to tolerate the chemically modified saccharide derivatives, and the size of chemical modification is ideally as small as possible.[10]

Yet, even the current alkyne/azide-based chemical reporters are still bulky for general applications.[11,12] For the metabolic glycoengineering of ManNAc salvage pathway with which researchers have so far found most success, the chemical reporters' steric hindrance hampers the monosaccharide derivative's metabolism by enzymes, recognition by transferases, and eventually disrupts their modification onto substrate proteins.[3,8,10,11,13] The most effective acetylmannosamine derivative found to date, ManNAz (Figure 1A), resulted in significantly less glycoprotein levels than the wild-type ManNAc and generated a low percentage of modified sialic acid in mammalian cell lines.[3,9,14,15] Even for cells eventually displaying modified sialic acids such as *N*-acetylneuraminic acid on the membranes, modification at the *N*-acetyl position with click chemistry tags or other functional groups resulted in reduced protein interactions and downstream biological activities.[16,17] More importantly, the peracetylated Ac_4ManNAz was revealed to incur growth inhibition and further cytotoxicity when administered to cell lines at concentrations higher than ∼100 μM.[7,18,19] Thus, metabolically more effective and safer ManNAc analogues with reduced steric are constantly needed, which would have a significant impact on the probing of cellular glycoconjugates' characteristics and functions.[7,20]

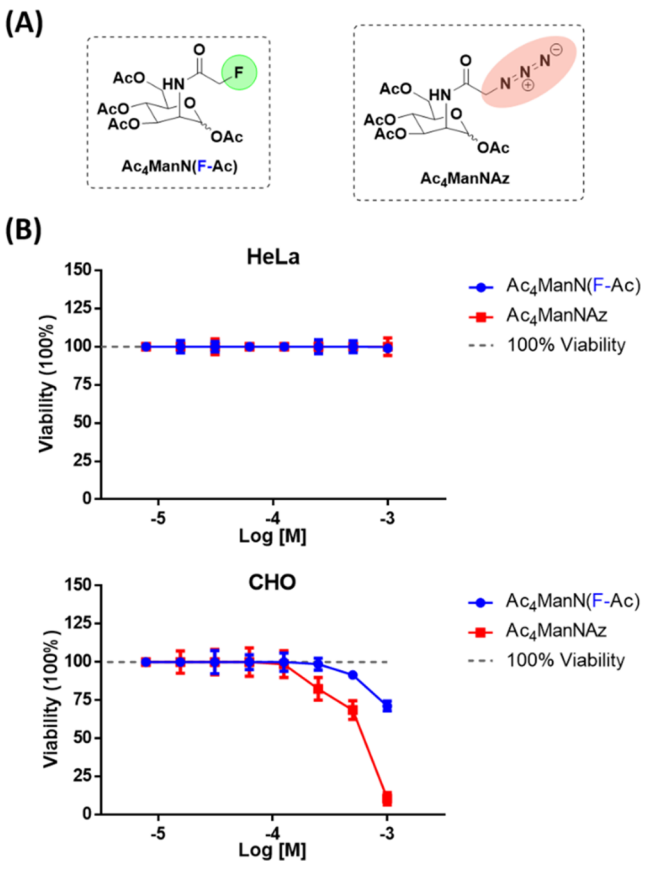

Figure 1. Cytotoxicity evaluation of the peracetylated *N*-acetylmannosamine derivatives. (A) Chemical structures of the α-fluorine-tagged monosaccharide Ac_4ManN(F-Ac) and Ac_4ManNAz. (B) Cytotoxicity of the peracetylated *N*-acetylmannosamine derivatives in HeLa or CHO cells after 48 h of incubation.

Given the fluorine atom's similarity in size to hydrogen and the minimal perturbance of fluorine substitutions to protein structure and function,[21−23] we have recently utilized the fluorine tag as a steric-free labeling approach to study post-translational modifications, specifically hijacking the acetylation process by multiple acetyltransferases with F-acetyl CoA.[12] We then invented a class of aryl thiol derivatized probes (Figure 2A) for a fluorine displacement reaction that is stable and bioorthogonal in mammalian cells.[12] The resulting TAMRA-SH and Biotin-SH probes enabled us to efficiently label, detect, and enrich acetylation protein substrates *in vitro* and in cells for chemical proteomics studies,[12,24] which cannot be achieved with traditional antibodies or "click chemistry"-based bulky chemical reporters.[12] This initial success on acetylation compelled us to apply this methodology toward glycosylation, starting with the most common mannosamine monosaccharide-based sialic acid synthesis and incorporation. Herein, we report our recent development of *N*-fluoroacetyl mannosamine (ManN(F-Ac))-mediated metabolic labeling, which, coupled with the aliphatic selenol-based new generation of fluorine displacement probes, has led to the efficient labeling of sialylated glycoconjugates in mammalian cell lines. More importantly, this fluorine-selenol displacement reaction (FSeDR) allowed us to sensitively probe the biological roles of sialylated glycoconjugates in cancer cell progression.

RESULTS AND DISCUSSION

Cytotoxicity Profile of the Peracetylated *N*-Fluoroacetyl Mannosamine

We started by preparing the tetraacetylated version of mannosamine, Ac_4ManNH_2 (**1**), following the reported Schiff base protection strategy (Scheme S1).[25] A subsequent amide coupling of the amino-mannosamine with sodium fluoroacetate resulted in the desired fluorine analogue, Ac_4ManN(F-Ac) (**2**), with an overall yield of ∼43% over four linear steps. Since peracetylated mannosamine derivatives were reported to affect cell growth and viability,[7,18,19] we compared the effects of Ac_4ManN(F-Ac) and Ac_4ManNAz on representative cell lines, including CHO cells, which are sensitive to mannosamine and sialic acid analogues.[26,27] As shown in Figure 1B, the commonly used azido analogue Ac_4ManNAz was nontoxic in HeLa cells but decreased the viability of CHO cells to ∼82 ± 7% and ∼68 ± 6% once incubated for 48 h at concentrations of 250 and 500 μM, respectively. On the contrary, Ac_4ManN-(F-Ac) (**2**) maintained a satisfactory viability of CHO cells at ∼99 ± 4% and ∼92 ± 3% at the corresponding concentrations of 250 and 500 μM, respectively. Thus, the fluorine-tagged Ac_4ManN(F-Ac) appears to possess a cytotoxicity profile

https://doi.org/10.1021/acsbiomedchemau.4c00084
ACS Bio Med Chem Au 2025, 5, 119−130

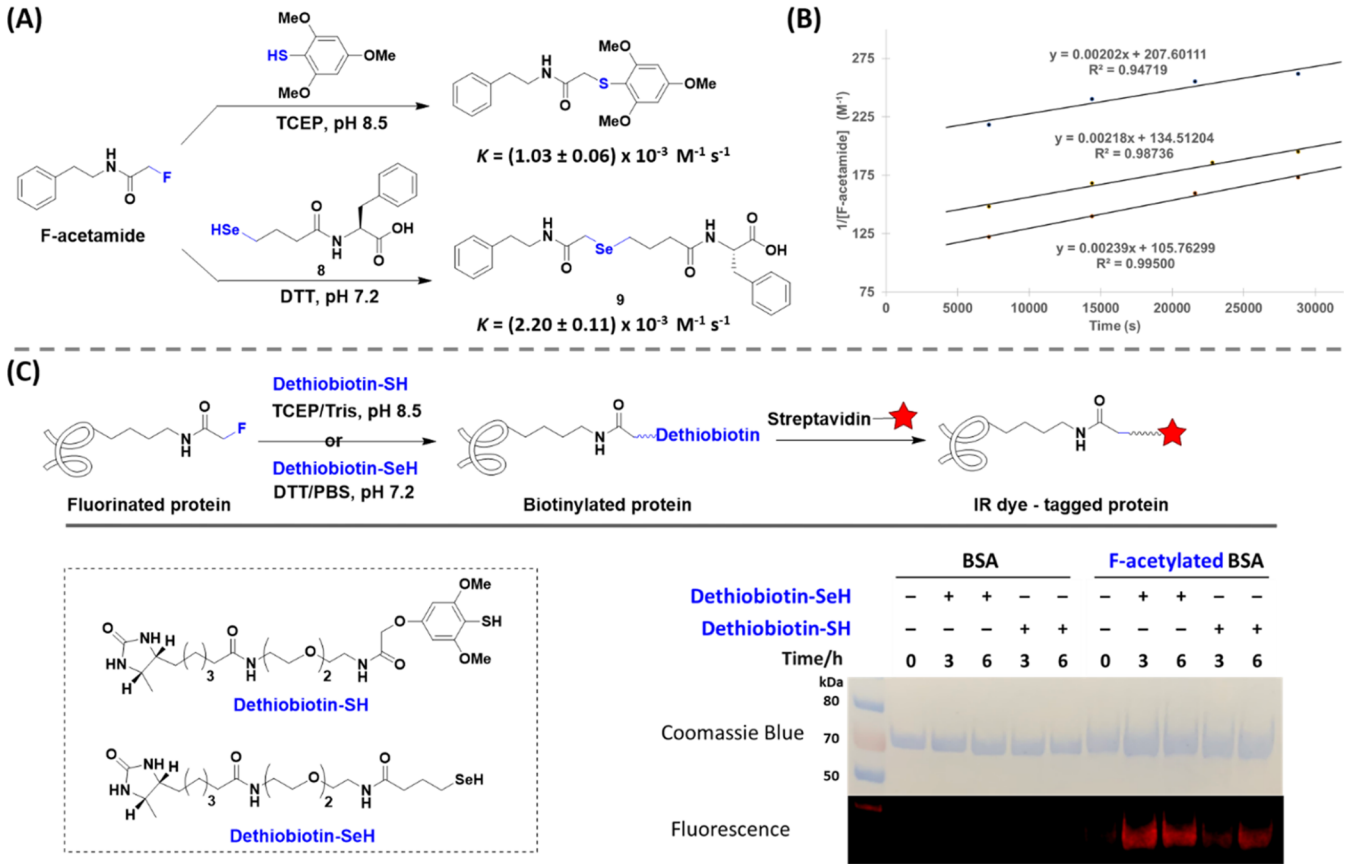

Figure 2. Characterization of the aliphatic selenol probe's fluorine displacement activity. (A) Model reactions between the fluoroacetamide substrate and each generation of fluorine displacement model warheads (aryl thiol, aliphatic selenol compound **8**). (B) Second-order reaction kinetics measurement of the model reaction between fluoroacetamide and the aliphatic selenol **8** at pH 7.2, in the presence of DTT. (C) Model BSA protein labeling with dethiobiotin-SH probe (pH 8.5, Tris buffer) or dethiobiotin-SeH probe (pH 7.2, PBS buffer). The fluorescent image is for the detection of IR dye-conjugated streptavidin that is incubated with the PVDF blot of the BSA protein following the probe labeling reaction. F-acetylated BSA was prepared by random lysine conjugation with a fluoroacetyl NHS ester.

better than that of the azido analogues and can be applicable to cell lines at concentrations below 500 μM.

Design, Synthesis, and Activation of the Aliphatic Selenol Probe

Previously, the aryl thiol probes, e.g., the 2,6-dimethoxybenzenethiol warhead, displaced fluorine from the α-fluoroacetamide functional group with a second-order reaction rate k of ~1.0×10^{-3} M^{-1} s^{-1}.[12] Nevertheless, this bioorthogonal reaction based on active thiols requires mildly basic conditions (pH ~ 8.5) to proceed, which we reasoned is likely due to the need for formation of more nucleophilic thiolates. Such a preference for anion formation in order to effectively displace fluorine led our attention to another element in the chalcogen family, selenium. Compared to thiol derivatives that mostly have pK_a values ~8−10,[12] the pK_a values for most selenols are ~5,[28−30] and they can be fully deprotonated at neutral pH to become selenolates, which have higher polarizability and are more nucleophilic than thiolates.[28] We therefore synthesized the aliphatic selenol model compound (**7**, Scheme S2) using selenocyanate as the protecting group and phenylalanine as the optically active unit to facilitate the monitoring of reactions.

To activate the precursor probe **7**, we attempted the deprotection of selenocyanate with sodium cyanoborohydride ($NaCNBH_3$), which turned out to be ineffective. On the other hand, treatment with five equivalents of sodium borohydride ($NaBH_4$) led to efficient reduction of **7** to the active selenol warhead **8** within just 10 min. We also observed that the selenol compound tends to readily form a dimer once upon exposure to air.[31] In order to determine the experimental conditions that can quickly convert diselenide back to the active monomer state, we explored tris(2-carboxyethyl) phosphine (TCEP), dithiothreitol (DTT), $NaCNBH_3$, and $NaBH_4$ as potential reducing agents. As shown in Figure S1, $NaBH_4$ rather than $NaCNBH_3$ can effectively reverse the formation of **8-dimer** within 30 min. Although commonly used as a strong reagent against oxidation in air, TCEP somehow also caused radical deselenization, resulting in the formation of the reported side-product TCEP = Se.[32] Meanwhile, DTT at ~25 equiv was observed to efficiently reduce **8-dimer** and the resulting monomer **8** remained active at ~10 mM for up to several hours. Compared with $NaBH_4$, DTT could be a milder reagent of choice for applications in biological systems. Hence, aliphatic selenol probes can be formulated as either protected selenocyanates or oxidized dimers for the purpose of long-term storage, which, right before application, can be activated in situ in a rapid manner through $NaBH_4$ or DTT, correspondingly.

Characterization of the Aliphatic Selenol Probe's *In Vitro* Activities

Next, we set out to evaluate the aliphatic selenol's fluorine displacement activities. The bimolecular reaction between **8** and the model substrate F-acetamide proceeded well at neutral pH (~7.2) and had an observed rate constant of (2.20 ± 0.11)

https://doi.org/10.1021/acsbiomedchemau.4c00084
ACS Bio Med Chem Au 2025, 5, 119−130

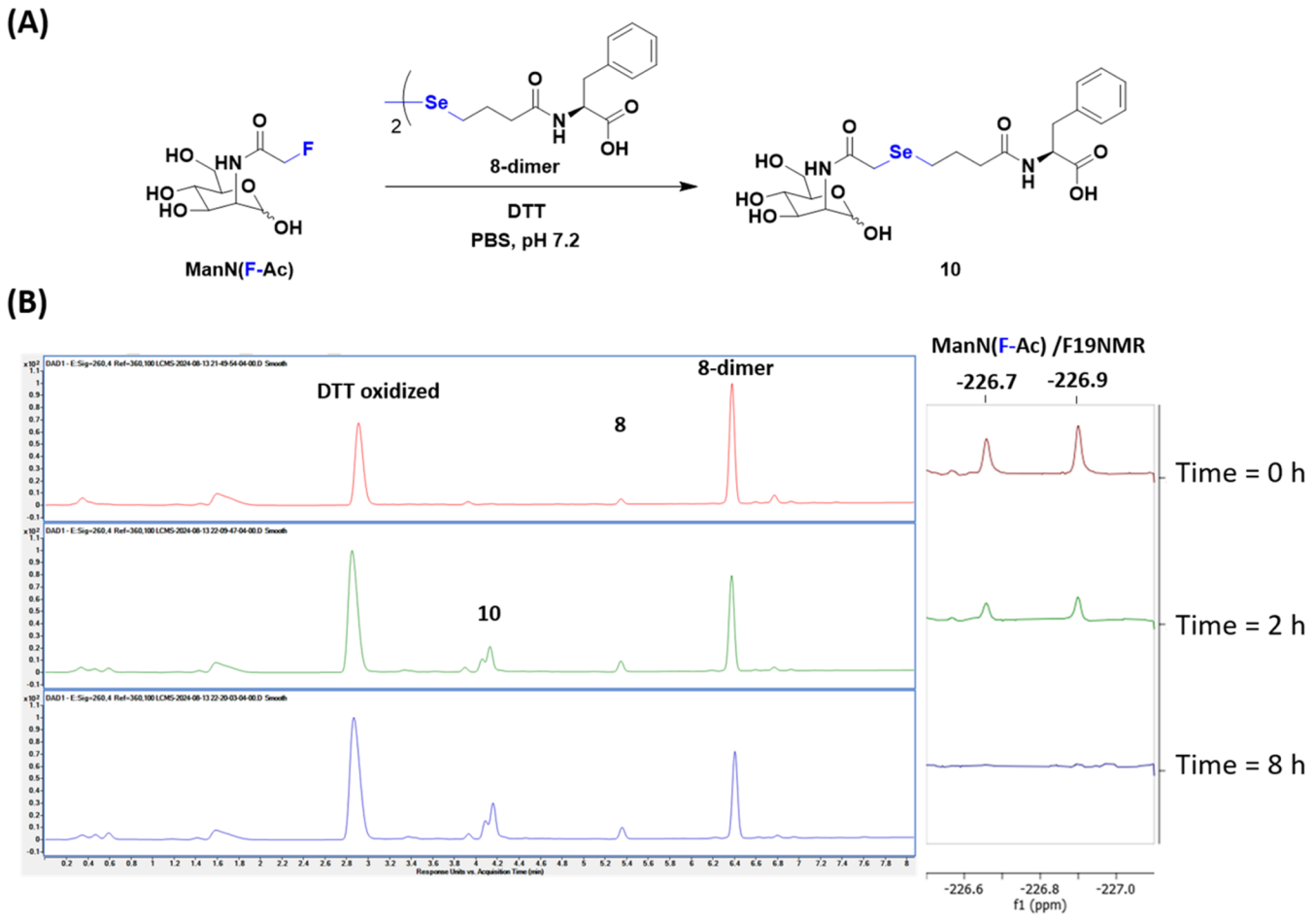

Figure 3. Time-dependent model fluorine displacement reaction on the *N*-fluoroacetyl mannosamine (ManN(F-Ac)) substrate by the aliphatic selenol warhead. (A) Chemical reaction scheme using **8-dimer** and DTT as the reducing agent in PBS buffer. (B) Time-dependent LC−MS and F19 NMR spectra of the reaction. For LC−MS, solvent A was water with 0.1% formic acid, and solvent B was acetonitrile with 0.1% formic acid. The elution started with 2.5% solvent B for the first 0.5 min at 1 mL/min, followed by gradient increase of solvent B to 95% from 0.5 to 6 min. For F19 NMR, the α and β anomers of ManN(F-Ac) were detected at −226.7 and −226.9 ppm.

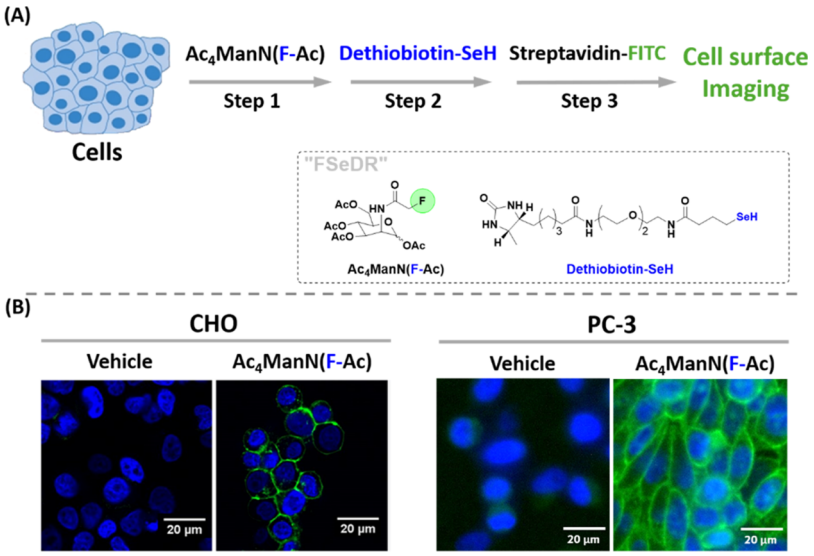

Figure 4. *N*-fluoroacetyl mannosamine-mediated metabolic labeling of sialic acids on mammalian cell surfaces. (A) Experimental scheme for cellular incorporation and metabolic labeling using the Ac_4ManN(F-Ac) and dethiobiotin-SeH toolkit. (B) Representative images of the labeled sialic acids (FITC, green) on the cell surfaces of the CHO and the PC-3 cell lines. Nuclei were stained with Hoechst (Blue).

https://doi.org/10.1021/acsbiomedchemau.4c00084
ACS Bio Med Chem Au 2025, 5, 119−130

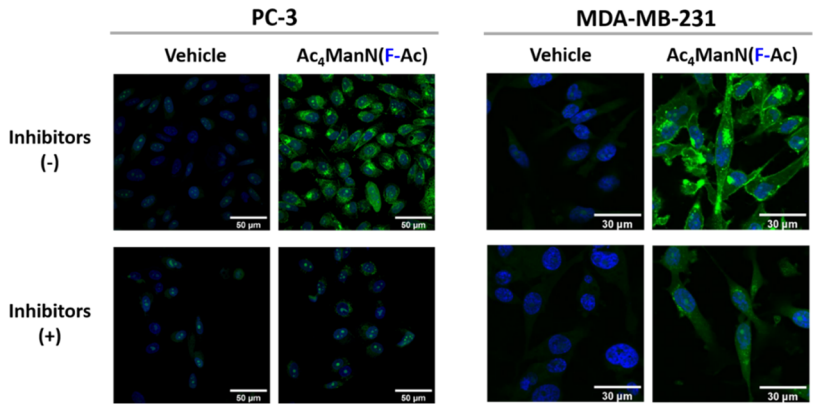

Figure 5. *N*-fluoroacetyl mannosamine-mediated metabolic intracellular labeling of protein substrates in the sialic acid biosynthesis pathway in representative mammalian cell lines (PC-3, MDA-MB-231). Samples in the bottom panels were preincubated with the noncompetitive *N*-acetylmannosamine kinase inhibitor (3-O-methyl-*N*-acetyl-D-glucosamine). The proteins labeled by dethiobiotin-SeH probe were detected inside the 0.1% Triton X-100 permeabilized cells with streptavidin-FITC (green). Nuclei were stained by Hoechst (Blue).

$\times 10^{-3}$ M^{-1} s^{-1} (Figure 2A,B), which is at least 2 times faster than the previous aryl thiol probe under basic reaction conditions.[12] We then furnished the aliphatic selenol warhead with a dethiobiotin functional handle through direct amide coupling (Scheme S4). The resulting dethiobiotin-SeH probe was compared side-by-side with the previously reported dethiobiotin-SH[12] in terms of labeling fluoroacetylated BSA model protein (Figure 2C). Efficient biotinylation by dethiobiotin-SeH occurred within 3 h of incubation at neutral pH, which appeared to reach saturation when the fluorescent intensities were compared with the sample BSA after 6 h of reaction. Nevertheless, little labeling by dethiobiotin-SH was detected within the first 3 h, and the fluorescent intensity was weak even after 6 h of labeling reaction by the thiol probe.

In order to gauge the potential of FSeDR-mediated labeling on fluorinated mannosamine metabolites, we utilized ManN-(F-Ac) as the model substrate (Scheme S3). Adopting the milder activation method discussed above, we incubated 3 equiv of **8-dimer** from the stock solution with ManN(F-Ac) in the presence of 25 equiv of DTT (Figure 3). The FSeDR conversion on ManN(F-Ac) turned out to be neat and clean (Figure 3B), with the desired product **10** accumulating within 2 h and showing mixed peaks of α/β isoforms at ∼4.2 min. Based on F19 NMR, the starting substrate ManN(F-Ac) was almost completely consumed after 8 h of reaction, and the targeted peak **10** appeared to be the only major product detected by LC−MS for this FSeDR reaction (full NMR and MS characterization for product **10** is available in the Supporting Information). Taken together, the aliphatic selenol probe seems to be efficient and specific for FSeDR reaction under physiological conditions.

N-Fluoroacetyl Mannosamine-Mediated Metabolic Labeling with the Aliphatic Selenol Probe

With the FSeDR toolkit in hand, we moved forward with metabolic glycoengineering as shown in Figure 4A. Mammalian cell lines were incubated with 150−200 μM peracetylated analogue Ac_4ManN(F-Ac) (**2**). The cells were fixed and then treated with dethiobiotin-SeH probe to initiate FSeDR-mediated labeling of the dethiobiotin tag onto the cell surface, which can be subsequently confirmed by staining with FITC-conjugated streptavidin for fluorescent detection. We observed clear fluorescent signals on the surface of the CHO cells (Figure 4B). Sialic acid has been reported to be upregulated in prostate cancer patient specimens,[33,34] and elevated levels of sialoglycoproteins have also been observed in prostate cancer cell lines such as PC-3.[35−37] Thus, we also attempted the metabolic engineering of sialylated glycoconjugates on the PC-3 cell line, which resulted in uniform global scale surface labeling. In either case, no sign of cytotoxicity was observed.

Encouraged by these results, we were curious about the intracellular level of sialoglycans and whether we could visualize the location of those sialylated glycoconjugates using the FSeDR toolkit. Sialic acid metabolism has been upregulated in hormone-sensitive cancer cells including PC-3 but also breast cancer cell lines such as MDA-MB-231.[38,39] Hence, PC-3 and MDA-MB-231 were separately cultured on imaging slides with or without the metabolic treatment of Ac_4ManN(F-Ac). After 2 days of incubation, cells were fixed, permeabilized, and again probed with dethiobiotin-SeH probe and streptavidin for fluorescent signal detection by confocal microscopy (Figure 5). For both prostate cancer cells and breast cancer cells, treatment with the FSeDR toolkit resulted in strong intracellular labeling across the cytoplasm and the punctate fluorescent signals could indicate the labeled sialoglycans in the Golgi apparatus, which is validated by our colocalization studies (Figure S2), showing most of the red fluorescent Golgi overlapped with the green fluorescence of sialoglycans and resulted in yellow colors within the merged images. This finding is consistent with the reported sialylation site and other lab's imaging observations.[40] Notably, confocal microscopic analysis of the cells treated with vehicle control gave very low background after reacting with the dethiobiotin-SeH probe, suggesting that the labeling of sialylated glycoconjugates is sensitive and specific. This is further confirmed by the parallel labeling and imaging analysis conducted with the presence of the ManNAc kinase inhibitor (3-*O*-methyl-*N*-acetyl-D-glucosamine),[41] which inhibits the biosynthesis of *N*-acetylneuraminic acid, and effectively blocked the tracking of sialoglycans in both PC-3 and MDA-MB-231.

Comparison of the Intracellular Metabolic Labeling between the *N*-Fluoroacetyl Mannosamine (FSeDR) Toolkit and the *N*-Azidoacetylmannosamine (CuAAC) Toolkit

Since the Ac_4ManNAz-based CuAAC toolkit is regarded as the gold standard in metabolic glycoengineering, we prepared the

https://doi.org/10.1021/acsbiomedchemau.4c00084
ACS Bio Med Chem Au 2025, 5, 119−130

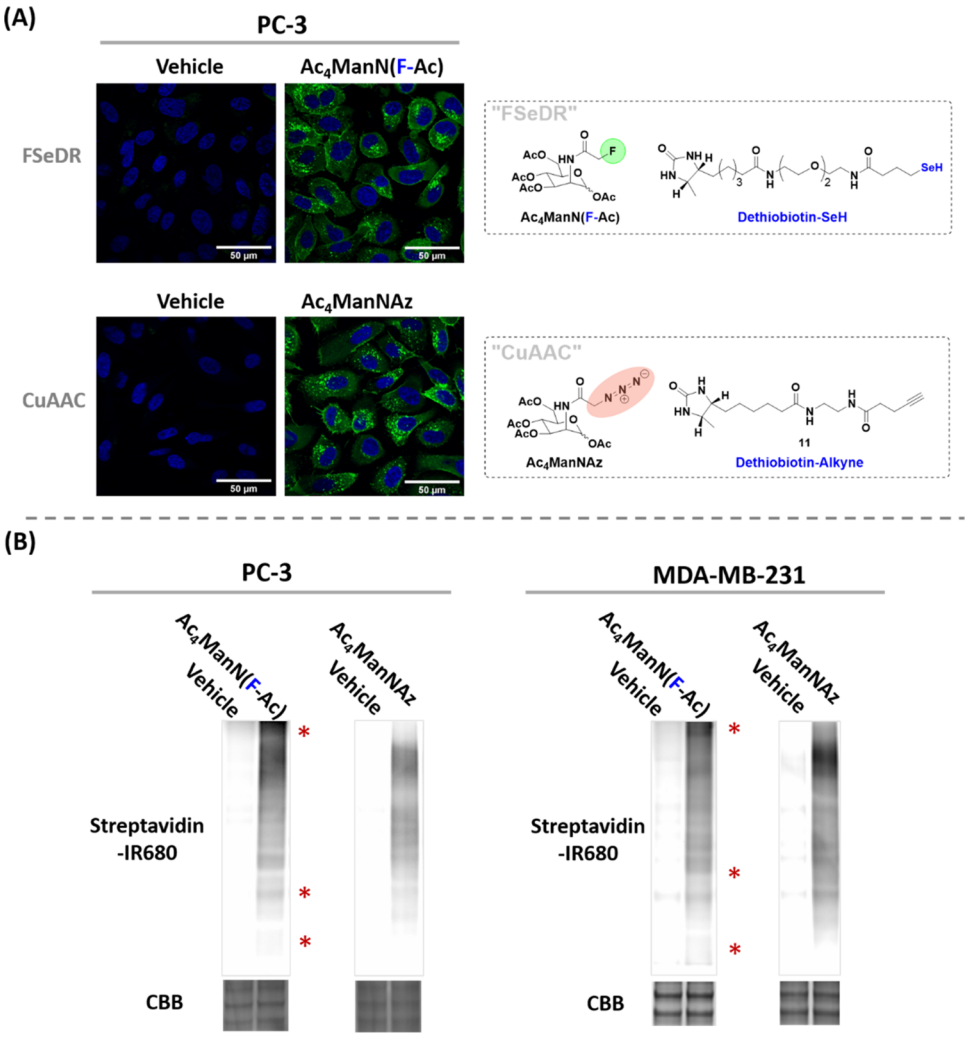

Figure 6. Comparison of the metabolic glycan labeling between the FSeDR and the "click chemistry" CuAAC toolkits. (A) Direct imaging results of PC-3 cell line using the pro-metabolite $Ac_4ManN(F\text{-}Ac)$ and $Ac_4ManNAz$, respectively. The cellular proteins labeled by dethiobiotin were visualized with streptavidin-FITC dye after Triton X-100-mediated permeabilization. (B) Corresponding cell lysates of PC-3 cells and MDA-MB-231 cells were each subjected to metabolic sialic acid labeling using FSeDR or CuAAC toolkits. The dethiobiotin-labeled proteins on the PAGE gels were detected via streptavidin-IR680 dye and visualized in the fluorescent channel. CBB is Coomassie brilliant blue staining as the loading control.

dethiobiotin-alkyne probe (Scheme S5) and pursued "click chemistry" labeling in parallel to the FSeDR-mediated metabolic labeling. Direct confocal microscopic imaging showed similar levels of fluorescence signals (Figure 6A) between these two methods. While the steric-free advantage of fluorinated mannosamine should lead to better hijacking of the metabolic biosynthesis, it is possible that the significantly faster reaction kinetics[42] of the "click chemistry"-based appendence with dethiobiotin compensated the weaker incorporation of azido-sialylated glycans. Nevertheless, PAGE gel analysis of those dethiobiotin-tagged proteins did reveal that the FSeDR approach has labeled more sialylated glycoproteins than did the CuAAC method (Figure 6B). For PC-3 cell lysates, the protein bands labeled and detected by FSeDR were apparently stronger in intensities than those labeled by CuAAC even for proteins migrating into the same molecular weight region. Notably, more protein labeling by FSeDR than CuAAC at high (>200 kDa) and low (<60 kDa) molecular weight ranges was observed in both PC-3 and MDA-MB-231 cells, as indicated by asterisks in Figure 6B, and being further confirmed by quantitative analysis in Figure S3. These results were consistent with the reported observations using traditional immunoaffinity methods that usually detected sialoglycoproteins at high and low molecular weights.[43,44] Therefore, the $Ac_4ManN(F\text{-}Ac)$-mediated FSeDR resulted in slightly better labeling of sialylated glycoconjugates than the traditional CuAAC method presumably due to the reduced steric hindrance of the F tag, and it theoretically should have more room to be further improved in the future depending on the continuous optimization of the FSeDR reaction kinetics. On a separate control run, we also observed almost completely diminished FSeDR labeling on the PC-3 cell lysates that had metabolized $Ac_4ManN(F\text{-}Ac)$ but were treated with sialidase before the addition of the dethiobiotin-SeH probe (Figure S4). This further confirms that the FSeDR labeling occurs accurately on sialylated cellular proteins.

https://doi.org/10.1021/acsbiomedchemau.4c00084
ACS Bio Med Chem Au 2025, 5, 119−130

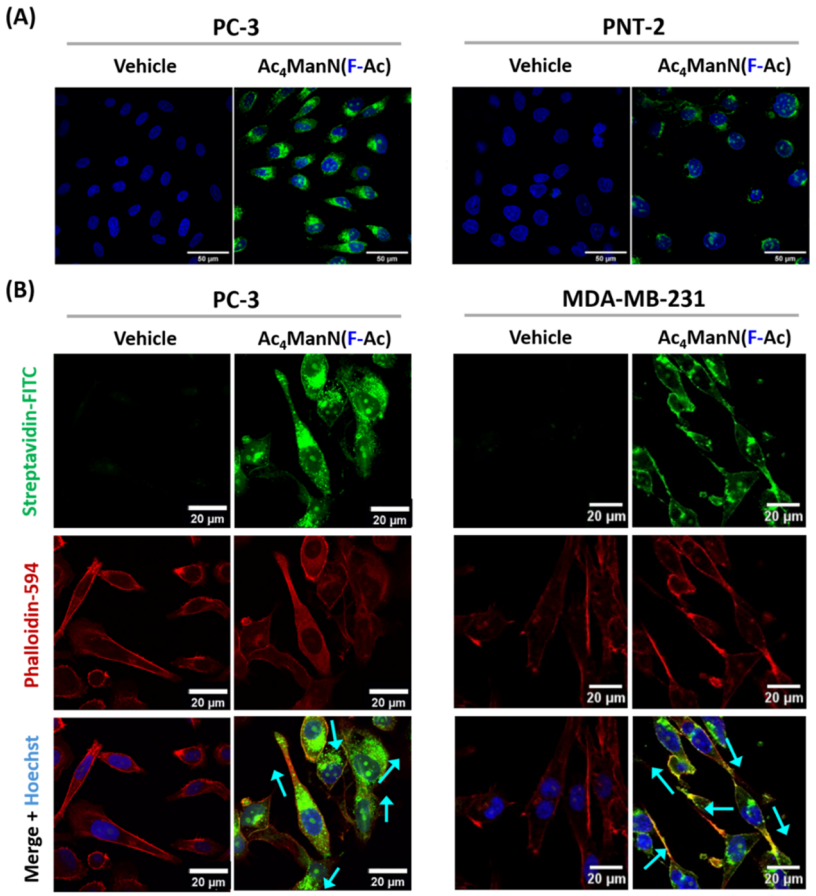

Figure 7. Probing the sialic acid regulation in cancer cell progression with the *N*-fluoroacetyl mannosamine-mediated metabolic labeling strategy. (A) Peracetylated ManN(F-Ac)- and FSeDR-based metabolic labeling of intracellular proteins (green) in the prostate cancer cell line (PC-3) and prostate tissue (PNT-2). Nuclei stained by Hoechst (blue). (B) Intracellular metabolic labeling of sialoglycoproteins (green) within migrating cancer cells such as PC-3 and MDA-MB-231. Actin was stained by phalloidin (red) while arrows (cyan) indicated the migration direction based on the actin-rich contact sites.

Metabolic Probing of Sialylated Glycoconjugates in Cancer Progression with *N*-Fluoroacetyl Mannosamine-Based FSeDR Toolkit

Hypersialylation is consistently observed in cancer cells,[36] including prostate cancer cell lines, which have overexpressed sialoglycans such as Lewis antigens and sialyl-T antigens that are favorable for tumor dissemination.[36−38] To detect this distinguished expression, we performed parallel metabolic labeling of both prostate cancer and tissue cell lines with Ac_4ManN(F-Ac) (Figure 7A). Compared to PC-3, a metastatic cancer cell line, the regular prostate tissue cell line PNT-2 indeed demonstrated significantly lower signal after the FSeDR reaction with the dethiobiotin-SeH probe. Notably, hypersialylation has also been linked to the metastatic spread of hormone-sensitive cancer cells, which overexpressed sialylated glycoconjugates but also certain sialyltransferases.[36,38,45] It is believed that surface sialylation changes are positively correlated with the metastatic potential of both prostate cancer and breast cancer.[35,37−39] Yet, little experimental evidence has been achieved with metabolic glycoengineering to visualize this glycan redistribution except for one reported study on melanoma cells.[46] With the application of the FSeDR labeling onto these hormone-sensitive and metastatic cell lines, we focused on the migrating cells as shown in Figure 7B. Under the confocal microscopic analysis, significant surface but also intracellular redistribution of sialylated glycoconjugates were captured in both PC-3 and MDA-MB-231 cells. Our results were pretty consistent with the reported sialylation redistribution during melanoma cell migration.[46] The accumulation of sialoglycoproteins mostly overlapped with the actin-rich contact sites and aligned well with the cell protrusion and migration directions as being indicated by the cyan arrows from the cell center to the lamellipodia (Figure 7B), suggesting the potential roles of the hypersialylation in promoting cancer cell adhesion and specifically the formation of filopodia.

CONCLUSIONS

In summary, we have explored and demonstrated the successful use of *N*-fluoroacetyl mannosamine as a pro-metabolite mimic of ManNAc. The aliphatic selenol warhead has been introduced here as the second-generation fluorine displacement probe that functions with enhanced reaction kinetics but also under improved reaction conditions for applications within physiological environment, i.e., the neutral pH range. The resulting FSeDR toolkit empowers successful metabolic glycoengineering, hijacking the sialic acid biosynthesis pathway in a more comprehensive and efficient manner than that using the traditionally used CuAAC toolkit. More importantly, the FSeDR-based metabolic labeling validated the upregulation of sialylated glycoconjugates in hormone-sensitive cancer cell lines and confirmed their spatial distribution during cancer progression and migration. Although the *N*-fluoroace-

https://doi.org/10.1021/acsbiomedchemau.4c00084
ACS Bio Med Chem Au 2025, 5, 119−130

tamide derivatization has been utilized on related sialic acid analogues,[47,48] our results here have been the very first report of α-fluorination on *N*-acetylmannosamine to probe the ManNAc/sialic acid salvage pathway. Moreover, the FSeDR-based fluorine displacement probes, such as dethiobiotin-SeH, efficiently converted *N*-fluoroacetamide to other biologically useful reporter groups such as biotin and potentially fluorophores, thereby empowering a much broader and more facile interrogation of sialylated glycoproteins than those in other *N*-fluoroacetamide derivatization studies. Current efforts are focused on the identification and functional annotation of these observed sialoglycoproteins and the systematic elucidation (including quantitative analysis) of their functional roles in cancer progression. Future work would involve the methodological invention toward metabolic glycoengineering of other important monosaccharides such as GalNAc and GlcNAc. It is also necessary to further design and evolve fluorine displacement probes with continuously improved reaction kinetics and bioorthogonality, which hopefully will lead to the real-time application of FSeDR in live cells.

MATERIALS AND METHODS

Chemical Probe Preparation

Reagents and solvents were purchased from commercial resources such as VWR, Fisher Scientific, Sigma-Aldrich, and Ambeed and were used directly without further purification. Analytical TLC was carried out with Silica Gel 60 F_{254} plates (Sorbent Technologies, Inc.). The chemicals on TLC were either visualized by UV 254 nm (UV lamp, Chemglass Life Sciences) or stained by phosphomolybdic acid or $KMnO_4$ oxidation. Compound purification was performed by flash column chromatography on columns manually loaded with silica gel grade 60 (230−400 mesh, Fisher Scientific) or by reverse-phase Combi-Flash on prepacked C18 columns (Teledyne ISCO). Further purification by preparative high-performance liquid chromatography (HPLC) was implemented on the Waters 1525 series that consists of a 2489 UV/vis detector, 1525 binary pump, and an XBridge Prep C18 column. Routine mass spectrometry analysis was done using a liquid chromatography−mass spectrometry (LC−MS) Agilent 6100. High-resolution LC−MS analysis was performed on an Agilent 6520 Accurate-Mass Quadrupole Time-of-Flight (Q-TOF) instrument coupled with an electrospray ionization source. For NMR analysis, ^{1}H NMR and ^{13}C NMR spectra were recorded on 400 or 500 MHz Bruker Advance, with tetramethylsilane (TMS) as the internal reference standard. The raw data were processed with MestReNova, and the chemical shifts were reported in parts per million (ppm) downfield from the internal standard (TMS). F19 NMR was acquired by placing the FSeDR model reaction mixture in a regular NMR tube within a Bruker spectrometer (471 MHz) equipped with an F19 probe (PA BBO 500S2 BBF-H-D-05 Z SP). The receiver gain was set to 191.1. A relaxation delay of 13.0 s and an acquisition time of 0.8738 s were used. Each spectrum took 240 accumulated scans. All of the related synthetic and reaction schemes produced for compound synthesis, and compound characterizations are available in the Supporting Information.

Measurement of the Reaction Kinetics

Reaction kinetics with the selenol model probe **8** was evaluated according to the reported method[49,50] and also following our own previously reported procedures.[12] Compound **8**, after cyano-deprotection from precursor **7**, was equally mixed with the substrate α-fluoroacetamide in 500 μL of PBS buffer (pH 7.2)/acetonitrile at concentrations of 5, 7.5, and 10 mM each. The final mixture also contained 20 equiv of DTT to maintain the reductive environment for the selenol monomer. The reaction was incubated at 37 °C, with 2 μL of the mixture withdrawn at the desired time points (120, 240, 360, and 480 min) and quenched with 0.5% TFA/acetonitrile. The samples were eventually analyzed by LC−MS, and the concentrations of the reactants ($[X]_t$ at time t, $[X]_0$ at time 0 for either reactant) were determined by comparing the ratios of peak areas with those from the standard curves. The rate constant (k) was determined by plotting $1/[X]_t$ (X is the substrate) against time and with the second-order equation ($1/[X]_t = 1/[X]_0 + kt$).

Cell Culturing

The CHO, PC-3, MDA-MB-231, and PNT-2 cell lines were all purchased from ATCC, and they were routinely authenticated. PC-3 cells were maintained in the 1:1 DMEM/F12 medium premixed with L-glutamine and HEPES (Cytiva HyClone). CHO and MDA-MB-231 cells were cultivated in DMEM high-glucose medium (Corning). PNT-2 cell line was cultured in RPMI 1640 media with L-Glutamine (Corning). All cell culture media were added with 10% FBS (Corning) and 1× antibiotic/antimycotic cocktail (100 IU/mL penicillin, 100 μg/mL streptomycin); and all cell lines were cultured in a humidified incubator at 37 °C with 5% CO_2.

Cytotoxicity Assay

Cytotoxicity evaluation was performed following our previously published procedures.[12] Briefly, the fluorinated and the azido-derivatized peracetylated mannosamine were each incubated with the mammalian cell lines at 2-fold serially diluted concentrations down from 1 mM. After incubation at 37 °C, 5% CO_2 for 48 h, the number of viable cells was quantified using CellTiter-Glo assay (Promega, WI), and the luminescent signals were recorded on the H1 Synergy plate reader (Biotek, Agilent).

Fluorine-Displacement-Based Labeling of Model Protein Bovine Serum Albumin (BSA)

Fluoroacetylated BSA (F-acetylated BSA) was prepared chemically by reacting 400 μL of BSA (2.4 mg/mL in DPBS, pH 7.2) with 14.8 μL of NHS-fluoroacetate (20 mM stock in DMSO) at room temperature for 2 h. The fluorinated BSA was purified by cold methanol precipitation to remove unconjugated fluoroacetate linkers, and then, the pellet was redissolved in 300 μL of water (2.6 mg/mL, ∼39 μM).

Labeling with the Dethiobiotin-SH probe. Approximately, 8 μL of F-acetylated BSA (39 μM stock in water) was mixed with 4 μL of TCEP (100 mM stock in water), 2 μL of dethiobiotin-SH (20 mM stock in DMSO), 1 μL of Tris buffer (1 M stock), and 5 μL of NaOH (200 mM stock in water). The final reaction volume was 20 μL, and the pH value of the mixture was 8.5. The reaction mixture was incubated at 37 °C for the indicated time point (0, 3, and 6 h), collected, and immediately snap frozen. The samples were stored at −80 °C until further analysis.

Labeling with the Dethiobiotin-SeH probe. Approximately, 2 μL of dethiobiotin-SeCN probe **7** (20 mM stock in CH_3CN) was mixed with 1 μL of $NaBH_4$ (200 mM stock in water) at room temperature for 10 min. The activated probe solution was then mixed with 4 μL of DTT (100 mM stock in water), 5 μL of PBS (250 mM stock in water), and 8 μL of F-acetylated BSA (39 μM stock in water). The final solution had a volume of 20 μL and a pH value of 7.2. The rest of the procedures, such as sample collections and storage, were the same as those mentioned above for the dethiobiotin-SH probe.

Gel analysis of the labeling results. Approximately, 6 μL of each sample after labeling with either probe and for different time points were loaded onto an 8% Bis-Tris SDS-PAGE with the MES-SDS running buffer (GenScript) for electrophoresis, which was later transferred onto PVDF membranes by a Trans-Blot SD semi dry transfer cell (Bio-Rad). The transfer was completed under 20 V voltage for 1.3 h in 1× NuPAGE transfer buffer (Invitrogen). The blot was blocked for 1 h with biotin-free casein buffer (Sigma-Aldrich) or self-prepared blocking buffer (3% BSA, 0.1% TBST, pH 8.0) and stained with streptavidin-IR Dye 680RD (LI-COR) at a dilution of 1/2000 for 1 h, followed by 3 times washings with 0.1% TBST (pH 8.0). The biotinylated proteins on the blot were detected by the LI-COR Odyssey Fc Imaging System (700 nm channel, Ex 685 nm/Em 730 nm). At the end, the blot was stripped with stripping buffer (Thermo Scientific) and stained with Coomassie brilliant blue (CBB) to show an equal loading amount of each sample

https://doi.org/10.1021/acsbiomedchemau.4c00084
ACS Bio Med Chem Au 2025, 5, 119−130

Metabolic Labeling of Sialylated Glycoconjugates on Mammalian Cell Surfaces

Approximately, 6×10^5 mammalian cells per well were seeded in six-well plates (Fisher Scientific). Once reaching 80% confluency, the cells were treated with the monosaccharide pro-metabolite by adding into each well 2 mL of fresh culture media that was premixed with 4 μL of 100 mM Ac_4ManN(F-Ac) (in DMSO as the stock solution) or 4 μL of DMSO (Corning) as vehicle control. After 48 h cell cultivation, the cells were rinsed with 1 mL of PBS buffer (Corning) three times and incubated with ∼4% paraformaldehyde solution (Electron Microscopy Sciences). Following the fixation at room temperature for 20 min, the cell samples were washed in 0.5 mL of PBS buffer three times to remove fixative additives.

For the labeling with the FSeDR-based dethiobiotin-SeH probe, 4 μL of freshly made 500 mM $NaBH_4$ aqueous solution was mixed with 2 μL of 200 mM dethiobiotin-SeCN probe in 30% acetonitrile and incubated within an Eppendorf tube for 10 min at room temperature. Alternatively, 4 μL of freshly prepared 1 M DTT was mixed with 2 μL of 100 mM dethiobiotin-SeH dimer (**8**-dimer) in 30% acetonitrile and was incubated at room temperature for 10 min. Then, 40 μL of 10× PBS buffer (Corning) and 360 μL of water were added and vortexed to mix. The pH of the activated probe solution was adjusted to ∼7.2 by 0.5 M NaOH aqueous solution. The cells were added with 100 μL of the probe solution per well and the mixtures were incubated for 8 h at 37 °C.

Right after this labeling reaction, cells in every well were washed with 100 μL of PBS buffer three times for 10 min each, followed by a one h incubation in 100 μL of blocking buffer (3% BSA, PBS, pH 7.2) at room temperature. The cell samples were finally stained with streptavidin-FITC (BD Pharmingen) and Hoechst 33342 dye that were dissolved in the cell-blocking buffer, for one h in the dark. The samples were subjected to three PBS washings for 20 min each and were resuspended in PBS for imaging analysis with confocal or epi-fluorescent microscope.

Metabolic Labeling and Probing of Sialylated Glycoconjugates Intracellularly

For Studies Only Employing the Dethiobiotin-SH Probe-Based FSeDR Labeling. Approximately, 3×10^4 cells per well were seeded in 8-well chambered slides (Cellvis). Once reaching 80% confluency, cells were treated with 300 μL of fresh media that was premixed with 0.45 μL of Ac_4ManN(F-Ac) stock solution (100 mM in DMSO) or the vehicle control (DMSO) and were incubated in a humidified incubator at 37 °C with 5% CO_2. For the comparison of labeling within the same cell line with or without the sialic acid biosynthesis inhibitor, approximately 4.69 μL of 3-*O*-methyl-GlcNAc stock solution (128 mM in DMSO, Cayman Chemical) or the DMSO control was also mixed with the media in addition to the monosaccharide. For comparison of metabolic labeling between PC-3 cells and PNT-2 cells, the media used for the two cell lines were the same (RPMI 1640 with the standard supplements as mentioned above).

After 2 days of metabolic incubation, the cells were rinsed with 300 μL of PBS buffer three times and then fixed in 175 μL of ∼4% paraformaldehyde PBS solution at room temperature for 20 min. Then, 300 μL of PBS buffer per well was used to wash for three times, 10 min each, to remove fixative additives. In parallel to this, around 13.2 μL of freshly prepared $NaBH_4$ aqueous solution (500 mM) was mixed with 6.6 μL of dethiobiotin-SeCN probe (200 mM, 30% acetonitrile/water) and incubated for 10 min at room temperature. Alternatively, 13.2 μL of DTT (1 M) was incubated with 6.6 μL of the dethiobiotin-SeH dimer (8-dimer probe, 100 mM) in 30% acetonitrile for 10 min. The activated probe solution was further mixed with 33 μL of a 1 M DTT stock solution, 66 μL of 10× PBS buffer (Corning), and 541 μL of water. The final probe mixture was adjusted with 0.5 M NaOH aqueous solution to ensure the pH value was ∼7.2. Each cell sample well was subsequently added with ∼160 μL of the above-mentioned probe solution. Then, the chamber was covered with a sticky sealing film and kept in an incubator at 37 °C for 8 h.

Following the FSeDR labeling, cells in each chamber well were first washed with 160 μL of 20 mM DTT/PBS solution (pH 7.2) at room temperature. After this, each well was washed with 300 μL of PBS buffer twice for 10 min to remove unreacted probes. Then, the cell samples were permeabilized at room temperature for 10 min with 200 μL of 0.1% Triton X-100 containing PBS, followed by three washings with 300 μL of PBS buffer (10 min each). The cells were then blocked by a one h incubation in 200 μL of cell-blocking buffer (3% BSA, PBS, pH 7.2) at room temperature. The blocked cells were eventually stained with streptavidin-FITC (1:200 dilution, BD Pharmingen) and Hoechst 33342 dye (1:1000 dilution) in the cell-blocking buffer for one h in the dark. For the samples with F-actin detection, CoraLite594-Phalloidin (1:200 dilution, Proteintech) was also added to the combined cell staining solution. For the samples for colocalization studies, Golgi was detected by rabbit anti-giantin antibody (BioLegend, 1:500 dilution) followed by the DyLight 649 Donkey anti-rabbit IgG (BioLegend, 1:500 dilution). Each incubation step took 1.5 h at room temperature, followed by PBS washing for 3 times at 10 min each time. After staining, the cell samples were subjected to 3× PBS washings for 20 min each and were stored at 4 °C in the dark until analysis by the confocal microscope.

For Imaging Studies Comparing FSeDR Labeling with CuAAC Labeling. Similar to the addition of Ac_4ManN(F-Ac), approximately 0.45 μL of azido-derivatized Ac_4ManNAz monosaccharide (100 mM in DMSO) was added to the cells, reaching 80% confluency. The metabolic incubation period for cell lines parallelly treated with either of the mannosamine analogues was shortened to 12 h, after which the cell samples metabolizing Ac_4ManNAz were rinsed and subjected to CuAAC-based labeling by the dethiobiotin-Alkyne probe **14**. Specifically, 6.5 μL of 50 mM $CuSO_4$ stock solution and 6.5 μL of 50 mM BTTES (Sigma-Aldrich) stock solution were incubated together for 10 min at room temperature. Then, the mixture was added with 6.5 μL of 10 mM dethiobiotin-alkyne probe stock solution, 6.5 μL of freshly made 250 mM sodium ascorbate solution, 65 μL of 10× PBS buffer (pH 7.2), and 559 μL of Milli-Q water. The probe solution was instantly aliquoted and added at a volume of 160 μL per well to the cell samples previously treated with Ac_4ManNAz. The CuAAC cellular labeling reaction was left at 37 °C for 8 h as well to be consistent with FSeDR labeling. The subsequent staining and cellular imaging procedures are the same as those mentioned above for the FSeDR.

For Cell Lysate PAGE Analysis Comparing FSeDR Labeling with CuAAC Labeling. To ensure more sensitive detection of individual protein bands, around 6×10^5 cells per well were seeded in six-well plates (Fisher Scientific). Upon 80% confluency, cells were added with 1.5 mL of fresh culture media per well that was premixed with 3 μL of 100 mM Ac_4ManN(F-Ac) for FSeDR-based labeling, 100 mM Ac_4ManNAz for CuAAC-based labeling, or DMSO as the vehicle control. After 12 h incubation, the cell samples were rinsed with 1 mL of PBS per well three times and lysed by 200 μL/well of prechilled RIPA lysis buffer (25 mM Tris-HCl, 150 mM NaCl, 1% NP-40, 1% sodium deoxycholate, 0.1% SDS, pH 7.6) at 4 °C for 20 min with gentle shaking. Immediately after this, the lysates were transferred into Eppendorf tubes and gently mixed with 1.5 mL of cold methanol per tube, followed by overnight incubation at −80 °C for complete protein precipitation. The precipitated proteins were spun down at 15,000*g* for 5 min and redissolved in 50 μL of PBS that contained 1% SDS, with the exact protein concentrations measured by BCA assay (Pierce, Thermo Fisher).

For FSeDR labeling, approximately 0.9 μL of the dethiobiotin-SeCN probe (200 mM) was activated by 1.8 μL of freshly prepared $NaBH_4$ aqueous solution (500 mM) in 10 μL of water for 10 min at room temperature. Alternatively, 8-dimer stock solution (100 mM) can be treated with DTT (1.8 μL, 1 M) as mentioned before for conversion to the active monomer dethiobiotin-SeH. For each sample labeling, 2.9 μL of the activated selenol probe solution was aliquoted out and mixed with 2 μL of 1 M DTT stock solution, 2 μL of 10× PBS buffer (pH 7.2), and 0.5 μL of 0.25 M NaOH solution (to adjust the final pH to 7.2) as well as water to fill the total volume up to 20 μL. This final probe reaction solution was added with 40 μg of the

https://doi.org/10.1021/acsbiomedchemau.4c00084
ACS Bio Med Chem Au 2025, 5, 119−130

aforementioned lysates resulting from the cells that have metabolized Ac_4ManN(F-Ac). After incubation at 37 °C for 12 h, the labeling reaction was quenched by freezing the lysates at −80 °C. For the control experiment, the lysates from cells having metabolized Ac_4ManN(F-Ac) were incubated with neuraminidase (sialidase, MilliporeSigma) at 0.04 U/40 μg lysate proteins, pH 6.0 for 3 h at 37 °C, before addition with the final probe solution. For CuAAC labeling, 0.9 μL of $CuSO_4$ stock solution (50 mM) and 0.9 μL of BTTES stock solution (50 mM) were mixed with 11 μL of water and incubated at room temperature for 10 min. The mixture was then added with 0.9 μL of a 10 mM dethiobiotin-alkyne probe stock solution, 0.9 μL of freshly made 250 mM sodium ascorbate solution, and 9 μL of 10× PBS buffer (pH 7.2). After sufficient mixing, an aliquot of ∼5.2 μL final probe reaction solution was added into the Eppendorf tube, which contained 40 μg of the lysates mentioned above as prepared from cells that have metabolized Ac_4ManNAz. The total reaction volume in each tube was filled up to 20 μL with water, and the labeling reaction lasted for 12 h at 37 °C before being quenched by freezing the lysate samples at −80 °C.

On the day of gel analysis, all of the lysate samples resulting from either FSeDR or CuAAC labeling were thawed on ice at the same time. For each tube that contained 20 μL of the processed cell lysate sample, ∼3 μL of DTT stock solution (1 M) and ∼8 μL of 4× LDS gel loading buffer were added. After heat denaturation at 70 °C for 10 min, all of the samples were quickly loaded onto a 4−12% Bis-Tris SDS-PAGE with the MES-SDS running buffer (GenScript) for electrophoresis (70−80 min at 140 V). The gel was then fixed in 50% isopropanol/45% water/5% acetic acid for 15 min at room temperature, followed by washing with water three times (15 min each). With ∼15 mL of Western blot blocking buffer (3% BSA, 0.1% TBST, pH 8.0), the fixed gel was further blocked at room temperature for 1 h and was immediately stained with streptavidin-IRDye 680RD (1/3000 dilution, LI-COR) for 1 h. After a final washing with 0.1% TBST (pH 8.0) three times, the biotinylated proteins were detected by the Bio-Rad ChemiDoc System. The band intensities were quantified by using ImageJ software. Ultimately, the gel was stripped with the stripping buffer (1.5% glycine, 0.01% SDS, 1% Tween 20, pH 2.2) and stained with Coomassie brilliant blue (CBB) as the loading control.

■ ASSOCIATED CONTENT

Supporting Information

The Supporting Information is available free of charge at https://pubs.acs.org/doi/10.1021/acsbiomedchemau.4c00084.

Supplementary figures, schemes, and procedures for chemical synthesis, along with the compound characterizations. (PDF)

■ AUTHOR INFORMATION

Corresponding Author

Rongsheng E. Wang − *Department of Chemistry, Temple University, Philadelphia, Pennsylvania 19122, United States;* orcid.org/0000-0002-5749-7447; Phone: +1 215 2041855; Email: rosswang@temple.edu

Authors

Yue Zhao − *Department of Chemistry, Temple University, Philadelphia, Pennsylvania 19122, United States*

Zhigang Lyu − *Department of Chemistry, Temple University, Philadelphia, Pennsylvania 19122, United States*

Benjamin Prather − *Department of Chemistry, Temple University, Philadelphia, Pennsylvania 19122, United States*

Todd R. Lewis − *Department of Chemistry, Temple University, Philadelphia, Pennsylvania 19122, United States*

Jinfeng Kang − *Department of Chemistry, Temple University, Philadelphia, Pennsylvania 19122, United States;* orcid.org/0000-0002-9408-4799

Complete contact information is available at: https://pubs.acs.org/10.1021/acsbiomedchemau.4c00084

Author Contributions

†Y.Z. and Z.L. made equal contributions to this work. Y.Z.: data curation, formal analysis, investigation, methodology, validation, and visualization; Z.L.: data curation, formal analysis, investigation, methodology, validation, and visualization; B.P.: data curation, formal analysis, investigation, methodology, and writing—review and editing; T.R.L.: data curation, methodology, validation, visualization, and writing—review and editing; J.K.: data curation, methodology, validation, and visualization; R.E.W.: conceptualization, data curation, formal analysis, funding acquisition, investigation, methodology, project administration, resources, supervision, validation, visualization, writing—original draft, and writing—review and editing. CRediT: **Yue Zhao** data curation, formal analysis, investigation, methodology, validation, visualization; **Zhigang Lyu** data curation, formal analysis, investigation, methodology, validation, visualization; **Benjamin Prather** data curation, formal analysis, investigation, methodology, writing - review & editing; **Todd R Lewis** data curation, methodology, validation, visualization, writing - review & editing; **Jinfeng Kang** data curation, methodology, validation, visualization; **Rongsheng E. Wang** conceptualization, data curation, formal analysis, funding acquisition, investigation, methodology, project administration, resources, supervision, validation, visualization, writing - original draft, writing - review & editing.

Notes

The authors declare no competing financial interest.

■ ACKNOWLEDGMENTS

R.E.W. is a Cottrell Scholar of Research Corporation for Science Advancement, and the authors acknowledge support from the NIH NIGMS under Grant R35GM133468 and NCI Pilot Award P30 CA006927. J.K. is partially supported by the NSF under Grant CHE-2144075. Support for the NMR facility at Temple University by a CURE grant from the Pennsylvania Department of Health is gratefully appreciated. The authors also thank the help from Bojana Gligorijevic Lab (Temple Bioengineering) on the use of the confocal microscope system and the help from Dr. Beth Moscato on F19 NMR analysis.

■ REFERENCES

(1) Varki, A. Sialic acids in human health and disease. *Trends Mol. Med.* **2008**, *14* (8), 351−360.

(2) Gorenflos-López, J. L.; Schmieder, P.; Kemnitz-Hassanin, K.; Asikoglu, H. C.; Celik, A.; Stieger, C. E.; Fiedler, D.; Hinderlich, S.; Hackenberger, C. P. R. Real-time monitoring of the sialic acid biosynthesis pathway by NMR. *Chem. Sci.* **2023**, *14* (13), 3482−3492.

(3) Dold, J. E. G. A.; Wittmann, V. Metabolic Glycoengineering with Azide- and Alkene-Modified Hexosamines: Quantification of Sialic Acid Levels. *ChemBioChem* **2021**, *22* (7), 1243−1251.

(4) Dedola, S.; Ahmadipour, S.; de Andrade, P.; Baker, A. N.; Boshra, A. N.; Chessa, S.; Gibson, M. I.; Hernando, P. J.; Ivanova, I. M.; Lloyd, J. E.; Marin, M. J.; Munro-Clark, A. J.; Pergolizzi, G.; Richards, S. J.; Ttofi, I.; Wagstaff, B. A.; Field, R. A. Sialic acids in infection and their potential use in detection and protection against pathogens. *RSC Chem. Biol.* **2024**, *5* (3), 167−188.

(5) Du, J.; Meledeo, M. A.; Wang, Z.; Khanna, H. S.; Paruchuri, V. D.; Yarema, K. J. Metabolic glycoengineering: sialic acid and beyond. *Glycobiology* **2009**, *19* (12), 1382−1401.
(6) Wang, H.; Wang, R.; Cai, K.; He, H.; Liu, Y.; Yen, J.; Wang, Z.; Xu, M.; Sun, Y.; Zhou, X.; Yin, Q.; Tang, L.; Dobrucki, I. T.; Dobrucki, L. W.; Chaney, E. J.; Boppart, S. A.; Fan, T. M.; Lezmi, S.; Chen, X.; Yin, L.; Cheng, J. Selective in vivo metabolic cell-labeling-mediated cancer targeting. *Nat. Chem. Biol.* **2017**, *13* (4), 415−424.
(7) Almaraz, R. T.; Aich, U.; Khanna, H. S.; Tan, E.; Bhattacharya, R.; Shah, S.; Yarema, K. J. Metabolic oligosaccharide engineering with N-Acyl functionalized ManNAc analogs: cytotoxicity, metabolic flux, and glycan-display considerations. *Biotechnol. Bioeng.* **2012**, *109* (4), 992−1006.
(8) Jacobs, C. L.; Yarema, K. J.; Mahal, L. K.; Nauman, D. A.; Charters, N. W.; Bertozzi, C. R. Metabolic labeling of glycoproteins with chemical tags through unnatural sialic acid biosynthesis. *Methods Enzymol.* **2000**, *327*, 260−275.
(9) Luchansky, S. J.; Argade, S.; Hayes, B. K.; Bertozzi, C. R. Metabolic functionalization of recombinant glycoproteins. *Biochemistry* **2004**, *43* (38), 12358−12366.
(10) Wratil, P. R.; Horstkorte, R.; Reutter, W. Metabolic Glycoengineering with N-Acyl Side Chain Modified Mannosamines. *Angew. Chem., Int. Ed.* **2016**, *55* (33), 9482−9512.
(11) Liu, F.; Chen, H. M.; Armstrong, Z.; Withers, S. G. Azido Groups Hamper Glycan Acceptance by Carbohydrate Processing Enzymes. *ACS Cent. Sci.* **2022**, *8* (5), 656−662.
(12) Lyu, Z.; Zhao, Y.; Buuh, Z. Y.; Gorman, N.; Goldman, A. R.; Islam, M. S.; Tang, H. Y.; Wang, R. E. Steric-Free Bioorthogonal Labeling of Acetylation Substrates Based on a Fluorine-Thiol Displacement Reaction. *J. Am. Chem. Soc.* **2021**, *143* (3), 1341−1347.
(13) Parle, D. R.; Bulat, F.; Fouad, S.; Zecchini, H.; Brindle, K. M.; Neves, A. A.; Leeper, F. J. Metabolic Glycan Labeling of Cancer Cells Using Variably Acetylated Monosaccharides. *Bioconjugate Chem.* **2022**, *33* (8), 1467−1473.
(14) Ren, Y.; Qiang, Y.; Duan, X.; Li, Z. The distinct difference in azido sugar metabolic rate between neural stem cells and fibroblasts and its application for decontamination of chemically induced neural stem cells. *Chem. Commun.* **2020**, *56* (15), 2344−2347.
(15) Saxon, E.; Luchansky, S. J.; Hang, H. C.; Yu, C.; Lee, S. C.; Bertozzi, C. R. Investigating cellular metabolism of synthetic azidosugars with the Staudinger ligation. *J. Am. Chem. Soc.* **2002**, *124* (50), 14893−14902.
(16) Briard, J. G.; Jiang, H.; Moremen, K. W.; Macauley, M. S.; Wu, P. Cell-based glycan arrays for probing glycan-glycan binding protein interactions. *Nat. Commun.* **2018**, *9* (1), No. 880.
(17) Lenza, M. P.; Egia-Mendikute, L.; Antonana-Vildosola, A.; Soares, C. O.; Coelho, H.; Corzana, F.; Bosch, A.; Manisha, P.; Quintana, J. I.; Oyenarte, I.; Unione, L.; Moure, M. J.; Azkargorta, M.; Atxabal, U.; Sobczak, K.; Elortza, F.; Sutherland, J. D.; Barrio, R.; Marcelo, F.; Jimenez-Barbero, J.; Palazon, A.; Ereno-Orbea, J. Structural insights into Siglec-15 reveal glycosylation dependency for its interaction with T cells through integrin CD11b. *Nat. Commun.* **2023**, *14* (1), No. 3496.
(18) Kim, E. J.; Sampathkumar, S. G.; Jones, M. B.; Rhee, J. K.; Baskaran, G.; Goon, S.; Yarema, K. J. Characterization of the metabolic flux and apoptotic effects of O-hydroxyl- and N-acyl-modified N-acetylmannosamine analogs in Jurkat cells. *J. Biol. Chem.* **2004**, *279* (18), 18342−18352.
(19) Jones, M. B.; Teng, H.; Rhee, J. K.; Lahar, N.; Baskaran, G.; Yarema, K. J. Characterization of the cellular uptake and metabolic conversion of acetylated N-acetylmannosamine (ManNAc) analogues to sialic acids. *Biotechnol. Bioeng.* **2004**, *85* (4), 394−405.
(20) Oetke, C.; Brossmer, R.; Mantey, L. R.; Hinderlich, S.; Isecke, R.; Reutter, W.; Keppler, O. T.; Pawlita, M. Versatile biosynthetic engineering of sialic acid in living cells using synthetic sialic acid analogues. *J. Biol. Chem.* **2002**, *277* (8), 6688−6695.
(21) Tressler, C. M.; Zondlo, N. J. Perfluoro-tert-butyl Homoserine Is a Helix-Promoting, Highly Fluorinated, NMR-Sensitive Aliphatic Amino Acid: Detection of the Estrogen Receptor.Coactivator Protein-Protein Interaction by (19)F NMR. *Biochemistry* **2017**, *56* (8), 1062−1074.
(22) Mishra, N. K.; Urick, A. K.; Ember, S. W.; Schonbrunn, E.; Pomerantz, W. C. Fluorinated aromatic amino acids are sensitive 19F NMR probes for bromodomain-ligand interactions. *ACS Chem. Biol.* **2014**, *9* (12), 2755−2760.
(23) Gee, C. T.; Koleski, E. J.; Pomerantz, W. C. Fragment screening and druggability assessment for the CBP/p300 KIX domain through protein-observed 19F NMR spectroscopy. *Angew. Chem., Int. Ed.* **2015**, *54* (12), 3735−3739.
(24) Zhao, Y.; Zhao, M.; Lyu, Z.; Gorman, N.; Lewis, T. R.; Goldman, A. R.; Tang, H.-Y.; Wang, R. E. Steric-free bioorthogonal profiling of cellular acetylation and glycosylation via a fluorine-selenol displacement reaction (FSeDR), 2022. DOI: 10.1101/2022.09.13.507737.
(25) Biswas, N. N.; Yu, T. T.; Kimyon, O.; Nizalapur, S.; Gardner, C. R.; Manefield, M.; Griffith, R.; Black, D. S.; Kumar, N. Synthesis of antimicrobial glucosamides as bacterial quorum sensing mechanism inhibitors. *Bioorg. Med. Chem.* **2017**, *25* (3), 1183−1194.
(26) Yin, B.; Wang, Q.; Chung, C. Y.; Bhattacharya, R.; Ren, X.; Tang, J.; Yarema, K. J.; Betenbaugh, M. J. A novel sugar analog enhances sialic acid production and biotherapeutic sialylation in CHO cells. *Biotechnol. Bioeng.* **2017**, *114* (8), 1899−1902.
(27) Yin, B.; Wang, Q.; Chung, C. Y.; Ren, X.; Bhattacharya, R.; Yarema, K. J.; Betenbaugh, M. J. Butyrated ManNAc analog improves protein expression in Chinese hamster ovary cells. *Biotechnol. Bioeng.* **2018**, *115* (6), 1531−1541.
(28) Huber, R. E.; Criddle, R. S. Comparison of the Chemical Properties of Selenocysteine and Selenocystine with Their Sulfur Analogs (Reprinted from Archives of Biochemistry and Biophysics, vol 122, pg 164−173, 2022). *Arch. Biochem. Biophys.* **2022**, *726*, No. 109233.
(29) Krief, A.; Hevesi, L. *Organoselenium Chemistry I: Functional Group Transformations*; Springer-Verlag: Berlin, 1988; Vol. *xi*, p 221.
(30) Thapa, B.; Schlegel, H. B. Theoretical Calculation of pK(a)'s of Selenols in Aqueous Solution Using an Implicit Solvation Model and Explicit Water Molecules. *J. Phys. Chem. A* **2016**, *120* (44), 8916−8922.
(31) Pálla, T.; Mirzahosseini, A.; Noszal, B. Species-Specific, pH-Independent, Standard Redox Potential of Selenocysteine and Selenocysteamine. *Antioxidants* **2020**, *9* (6), 465.
(32) Dery, S.; Reddy, P. S.; Dery, L.; Mousa, R.; Dardashti, R. N.; Metanis, N. Insights into the deselenization of selenocysteine into alanine and serine. *Chem. Sci.* **2015**, *6* (11), 6207−6212.
(33) Zhang, C.; Yan, L.; Song, H.; Ma, Z.; Chen, D.; Yang, F.; Fang, L.; Li, Z.; Li, K.; Li, D.; Yu, N.; Liu, H.; Xu, Z. Elevated Serum Sialic Acid Levels Predict Prostate Cancer As Well As Bone Metastases. *J. Cancer* **2019**, *10* (2), 449−457.
(34) Michalakis, K.; Ilias, I.; Triantafyllou, A.; Polymeris, A.; Kastriotis, I.; Chairakaki, A. D.; Savopoulos, C. Detection of prostate cancer by sialic acid level in patients with non-diagnostic levels of prostate-specific antigen. *Maturitas* **2012**, *73* (4), 325−330.
(35) Yang, L.; Nyalwidhe, J. O.; Guo, S.; Drake, R. R.; Semmes, O. J. Targeted identification of metastasis-associated cell-surface sialoglycoproteins in prostate cancer. *Mol. Cell Proteomics* **2011**, *10* (6), No. M110-007294.
(36) Hugonnet, M.; Singh, P.; Haas, Q.; von Gunten, S. The Distinct Roles of Sialyltransferases in Cancer Biology and Onco-Immunology. *Front. Immunol.* **2021**, *12*, No. 799861.
(37) Bai, R.; Luan, X.; Zhang, Y.; Robbe-Masselot, C.; Brockhausen, I.; Gao, Y. The expression and functional analysis of the sialyl-T antigen in prostate cancer. *Glycoconjugate J.* **2020**, *37* (4), 423−433.
(38) Büll, C.; Stoel, M. A.; den Brok, M. H.; Adema, G. J. Sialic acids sweeten a tumor's life. *Cancer Res.* **2014**, *74* (12), 3199−3204.
(39) Teoh, S. T.; Ogrodzinski, M. P.; Ross, C.; Hunter, K. W.; Lunt, S. Y. Sialic Acid Metabolism: A Key Player in Breast Cancer Metastasis Revealed by Metabolomics. *Front. Oncol.* **2018**, *8*, 174.
(40) Hsu, T. L.; Hanson, S. R.; Kishikawa, K.; Wang, S. K.; Sawa, M.; Wong, C. H. Alkynyl sugar analogs for the labeling and

visualization of glycoconjugates in cells. *Proc. Natl. Acad. Sci. U.S.A.* **2007**, *104* (8), 2614−2619.
(41) Zeitler, R.; Giannis, A.; Danneschewski, S.; Henk, E.; Henk, T.; Bauer, C.; Reutter, W.; Sandhoff, K. Inhibition of N-acetylglucosamine kinase and N-acetylmannosamine kinase by 3-O-methyl-N-acetyl-D-glucosamine in vitro. *Eur. J. Biochem.* **1992**, *204* (3), 1165−1168.
(42) Lang, K.; Chin, J. W. Bioorthogonal Reactions for Labeling Proteins. *ACS Chem. Biol.* **2014**, *9* (1), 16−20.
(43) Srivastava, S.; Verhagen, A.; Sasmal, A.; Wasik, B. R.; Diaz, S.; Yu, H.; Bensing, B. A.; Khan, N.; Khedri, Z.; Secrest, P.; Sullam, P.; Varki, N.; Chen, X.; Parrish, C. R.; Varki, A. Development and applications of sialoglycan-recognizing probes (SGRPs) with defined specificities: exploring the dynamic mammalian sialoglycome. *Glycobiology* **2022**, *32* (12), 1116−1136.
(44) Surman, M.; Wilczak, M.; Przybylo, M. Lectin-Based Study Reveals the Presence of Disease-Relevant Glycoepitopes in Bladder Cancer Cells and Ectosomes. *Int. J. Mol. Sci.* **2022**, *23* (22), No. 14368, DOI: 10.3390/ijms232214368.
(45) Dobie, C.; Skropeta, D. Insights into the role of sialylation in cancer progression and metastasis. *Br. J. Cancer* **2021**, *124* (1), 76−90.
(46) Dommerholt, J.; Schmidt, S.; Temming, R.; Hendriks, L. J.; Rutjes, F. P.; van Hest, J. C.; Lefeber, D. J.; Friedl, P.; van Delft, F. L. Readily accessible bicyclononynes for bioorthogonal labeling and three-dimensional imaging of living cells. *Angew. Chem., Int. Ed.* **2010**, *49* (49), 9422−9425.
(47) Moons, S. J.; Adema, G. J.; Derks, M. T.; Boltje, T. J.; Bull, C. Sialic acid glycoengineering using N-acetylmannosamine and sialic acid analogs. *Glycobiology* **2019**, *29* (6), 433−445.
(48) Li, Y.; Yu, H.; Cao, H.; Lau, K.; Muthana, S.; Tiwari, V. K.; Son, B.; Chen, X. Pasteurella multocida sialic acid aldolase: a promising biocatalyst. *Appl. Microbiol. Biotechnol.* **2008**, *79* (6), 963−970.
(49) Sundhoro, M.; Jeon, S.; Park, J.; Ramstrom, O.; Yan, M. Perfluoroaryl Azide Staudinger Reaction: A Fast and Bioorthogonal Reaction. *Angew. Chem., Int. Ed.* **2017**, *56* (40), 12117−12121.
(50) Addy, P. S.; Erickson, S. B.; Italia, J. S.; Chatterjee, A. A Chemoselective Rapid Azo-Coupling Reaction (CRACR) for Unclickable Bioconjugation. *J. Am. Chem. Soc.* **2017**, *139* (34), 11670−11673.

https://doi.org/10.1021/acsbiomedchemau.4c00084
ACS Bio Med Chem Au 2025, 5, 119−130